Accelerating Effect of Umbelliferone on Peroxidase-Catalyzed Oxidation of Indole-3-acetic Acid at Neutral pH

Sergey N. Krylov* and H. Brian Dunford*

Department of Chemistry, University of Alberta, Edmonton, Alberta, Canada T6G 2G2

Received: August 14, 1996; In Final Form: October 12, 1996[⊗]

The acceleration by the phenol umbelliferone (7-hydroxycoumarin) of the horseradish peroxidase (HRP) catalyzed oxidation of indole-3-acetic acid (IAA) was studied at pH 7.4 using spectral and kinetic approaches. For the system 0.1 mM IAA/1 μM HRP/variable umbelliferone concentration, an increase in rate by a factor of 8 was reached in the presence of 1 μM umbelliferone; further increase of the umbelliferone concentration had no further effect. The rate constants for the peroxidase compounds I and II (HRP-I and HRP-II) reductions by umbelliferone in the absence of IAA were measured in the transient state as functions of the umbelliferone concentration. The plot of the pseudo-first-order rate constant k_{obs} vs [umbelliferone] for HRP-I reduction was curved upward. This result implies that umbelliferone catalyzes its own oxidation by HRP-I. The bimolecular rate constant of the reduction of 1 μM HRP-I by 1 μM umbelliferone was estimated to be 1.1×10^5 M^{-1} s^{-1}. The plot of k_{obs} vs [umbelliferone] was linear for HRP-II reduction, yielding a bimolecular rate constant of 1.7×10^5 M^{-1} s^{-1}. The influence of umbelliferone on the rates of HRP-I and HRP-II reduction by IAA was also studied. It was found that 1 μM umbelliferone accelerates the reduction of 1 μM HRP-I by a factor of 10 but did not influence the reduction of HRP-II by IAA. The influence of umbelliferone on the HRP-I reduction by umbelliferone and/or IAA suggests that HRP-I can bind umbelliferone at a site different from the active site, where it provides a beneficial conformational change. However, the binding of umbelliferone to native HRP was not observed. A detailed mechanism for the HRP-catalyzed oxidation of IAA, both in the absence and in the presence of umbelliferone, is presented. There are three umbelliferone-induced accelerating effects: (i) the reduction of the rate-limiting HRP species, HRP-II, by umbelliferone, which increases the rate of enzyme turnover and hence the rate of IAA oxidation, (ii) the nonenzymatic oxidation of IAA by free radicals of umbelliferone formed in the HRP-catalyzed oxidation of umbelliferone, and (iii) umbelliferone-induced acceleration of the HRP-I reduction by IAA. The magnitudes of these three effects are similar.

1. Introduction

Peroxidases are able to catalyze the oxidation of several substrates aerobically without added peroxide. Among these substrates are: indole-3-acetic acid (IAA),[1−8] NADH,[9] dihydroxyfumarate,[10] and isobutyraldehyde.[11] These peroxidase-catalyzed O_2-consuming processes are called peroxidase−oxidase reactions. Peroxidase−oxidase reactions are of interest to researchers because (i) they exhibit a number of nonlinear dynamic behaviors such as bistabilities, oscillations, and chaos,[7,9,12] (ii) they produce chemiluminescence,[11,13−15] and (iii) at least one of them (oxidation of IAA) is an important physiological reaction.[16] IAA is a phytohormone with many growth regulatory functions.[17] The peroxidase-catalyzed oxidation of IAA plays an important role in IAA catabolism *in vivo* and thus in control of plant growth.[18]

IAA oxidation by peroxidase is a very complex process in which many reaction intermediates and final products are formed.[19] Moreover, during the course of the reaction peroxidase is converted from the native enzyme into several catalytic and inactive forms.[5,20,21]

Two main reaction pathways for the oxidation of IAA have been recognized, labeled peroxidase and oxidase. In the classical peroxidase pathway, hydroperoxide (ROOH) is the two-electron-oxidizing substrate of the native enzyme, converting it into compound I. IAA is the one-electron-reducing substrate for both of the enzyme intermediates, HRP-I and HRP-II. A nonclassical part of the peroxidase pathway is a free radical chain reaction in which ROOH is regenerated.[2,5−8] The oxidase pathway involves the ferrous enzyme and HRP-III.[3] The substrate of Fe^{2+}−HRP is oxygen, and the substrate of HRP-III is IAA.[3,4] The pathway which is followed depends upon the experimental conditions. A high pH promotes the peroxidase pathway while a low pH favors the oxidase pathway.[3−5] In a very recent paper Gazaryan et al. suggested a relatively simple alternative mechanism for the HRP-catalyzed IAA oxidation.[22] They postulated that a ternary complex of native ferric HRP, IAA, and O_2 plays a key role in both the initiation step and subsequent reaction cycle. This provocative hypothesis is speculative, since there is no evidence for the ternary complex. However, it is certain to stimulate further work.

The mechanism of HRP-catalyzed IAA oxidation at neutral pH has been intensively studied for the past two years.[5−7] It was proven that IAA is oxidized by a combination of both the enzymatic cycle and a free radical chain reaction.[5] The enzymatic cycle produces free radicals of IAA required for sustaining a free radical chain, while a free radical chain reaction produces hydroperoxide needed for sustaining the enzymatic cycle. It was shown that the symbiotic effect of the enzymatic cycle and the free radical chain reaction is so efficient that no additional steps are required for the reaction initiation; the traces of hydroperoxide derived from IAA, which cannot be totally eliminated from the IAA solutions, are all that is required for

* To whom correspondence may be addressed. For S.N.K. phone (403) 492-9251, fax (403) 492-8231; e-mail skrylov@gpu.srv.ualberta.ca. For H.B.D. phone (403) 492-3818; fax (403) 492-8231; e-mail brian.dunford@ualberta.ca.

[⊗] Abstract published in *Advance ACS Abstracts,* December 1, 1996.

S0022-3654(96)02493-8 CCC: $12.00

the initiation.[6,7] The mechanism of the phenol-induced inhibition of the HRP-catalyzed IAA oxidation was also studied.[7] It was shown that phenolic inhibitors act mainly as competitive substrates of HRP-I and HRP-II. Free radical scavenging abilities of phenols also can contribute to the inhibition but at relatively high phenol concentrations. A detailed model of the HRP-catalyzed IAA oxidation has been developed[6] and applied to the analysis of phenol-induced inhibition.[7]

Candeias et al., in two recent papers,[23,24] carefully identified free radical species obtained in IAA oxidation and measured their redox potentials and, in one case, the acid ionization constant. They also measured several important rate constants. Their results can be used for further understanding the details of HRP-catalyzed IAA oxidation and in particular for the development of a detailed model of this reaction.

Despite significant progress in understanding the mechanism of HRP-catalyzed IAA oxidation at neutral pH, some proposals are still speculative, and several questions remain unanswered.[8] Umbelliferone is known to accelerate IAA oxidation.[25] However, nothing has been known about the mechanism of its action. Here we present an experimental study of the umbelliferone-induced acceleration of the HRP-catalyzed IAA oxidation at pH 7.4. We also present a detailed model for the HRP-catalyzed IAA oxidation, making use of recent results obtained by Candeias et al. The mechanism of umbelliferone-induced acceleration of the HRP-catalyzed IAA oxidation is explained as an extension of the detailed model.

2. Materials and Methods

2.1. Materials. HRP (RZ = 3.0), umbelliferone, and IAA were obtained from Sigma (St. Louis, MO), while the components of buffers (acetate, phosphate, tris- and bicarbonate) as well as ferric chloride and perchloric acid were purchased from Fisher Scientific (Fair Lawn, NJ). Prepurified nitrogen (99.999%) was obtained from Praxair (Mississauga, ON).

IAA was dissolved by prolonged stirring in hot water. The HRP concentration was determined spectrophotometrically using the extinction coefficient at 403 nm of 1.02×10^5 M^{-1} cm^{-1}.[26] Unless otherwise stated, solutions were prepared in 0.1 M pH 7.4 phosphate buffer using deionized water. The final volume of the reaction mixture was 1 mL for spectrophotometric experiments and 3 mL for oxygen consumption experiments. The reaction was initiated by the addition of enzyme. Unless otherwise indicated, prior to reaction initiation the solution of IAA was saturated with air; the initial oxygen concentration was about 250 μM.[27] The temperature was kept at 20.0 ± 0.5 °C.

2.2. Equipment. The absorption spectra and most of the kinetics were measured with a Beckman DU 650 spectrophotometer. Kinetics were corrected for lamp intensity drift during the period of measurements. Quartz cuvettes with 1 cm path length were used. Stopped flow experiments as well as fluorimetric experiments were made on a SX.17MV sequential stopped-flow spectrometer (Applied Photophysics, UK). Oxygen consumption was followed on a Yellow Springs Instrument Model 53 oxygen monitor (Yellow Springs, OH).

2.3. Determination of the Rate Constants. The rate constants k_{obs} for the reduction of HRP-I and HRP-II by umbelliferone were measured using the stopped-flow apparatus by following the absorbance changes at 411 nm (isosbestic point for HRP and HRP-II spectra) and 430 nm (isosbestic point between HRP and HRP-I spectra). HRP-I was prepared by mixing equimolar amounts of HRP and H_2O_2; HRP-II was prepared by mixing equimolar amounts of HRP, H_2O_2, and caffeic acid. Caffeic acid is completely oxidized under these conditions. Thus, it does not influence the kinetics of HRP-II reduction. Both HRP-I and HRP-II were stable for the duration of the kinetic measurements. The initial concentrations of HRP-I and HRP-II after mixing with uimbelliferone were 1 μM.

The rate constants k_{obs} for the reduction of HRP-I by IAA in the presence and in the absence of umbelliferone were measured as described in the previous paragraph. The rate constants for the reduction of HRP-II by IAA in the presence and in the absence of umbelliferone were measured in deoxygenated solution using the procedure described earlier.[5] A small amount of deoxygenated concentrated umbelliferone was added by syringe through the rubber cover at the beginning of the single-exponential part of HRP-II decay. The initial concentrations after mixing were 1 μM HRP, 0.1 mM IAA, and 1 μM umbelliferone.

Unless otherwise stated, an excess of IAA and umbelliferone was used in the reaction mixtures compared to the enzyme concentration. Therefore, for these cases the kinetics of HRP-I and HRP-II reactions were pseudo-first-order. The k_{obs} values were determined by single-exponential curve fitting with floating end point using the standard program "Origin" (Microcal Software). Bimolecular rate constants were determined from the slope of the plot of k_{obs} against substrate concentration, if a linear plot was obtained, or from the slope of the tangent to the curve of k_{obs} versus substrate concentration, if curvature was observed.

2.4. Colorimetric Determination of IAA Concentration. The Salkowski reagent was prepared by mixing 50 mL of perchloric acid (70%, w/w), 50 mL of H_2O, and 2 mL of 0.5 M $FeCl_3$.[28] To evaluate a time dependence of IAA concentration in the reaction mixture IAA/HRP (with or without umbelliferone), 1 mL aliquots of the reaction mixture were added to vials containing 2 mL of Salkowski reagent every 0.5 min after the reaction initiation. An absorbance was measured at 535 nm in 25 min after the addition of the reaction mixture to the Salkowski reagent. The concentration of IAA in the reaction mixture was determined using a calibration line (absorbance vs [IAA]).

2.5. Spectral Analysis of HRP Species in the IAA/HRP System. It was shown in our previous paper that HRP-III is not formed during HRP-catalyzed IAA oxidation at pH 7.4. In the present work the concentrations of native HRP, HRP-I, and HRP-II in the reaction mixture 0.1 mM IAA/1 μM HRP were calculated from the corresponding absorption kinetic traces measured at 397 nm (isosbestic point for HRP-I and HRP-II spectra), 411 and 430 nm, respectively. The following extinction coefficients were used: $\epsilon^{HRP}_{397\,nm} = 9.76 \times 10^4$, $\epsilon^{HRP-I}_{411\,nm} = 4.32 \times 10^4$, and $\epsilon^{HRP-II}_{397\,nm} = 7.11 \times 10^4$ M^{-1} cm^{-1}. The extinction coefficients were determined by the absorption measurements for precisely prepared 1 μM native HRP, HRP-I, and HRP-II (The procedures for HRP-I and HRP-II preparations are in section 2.3.)

2.6. Spectral Analysis of the HRP Species in the IAA/HRP/Umbelliferone System. It was suspected that in the IAA/HRP/umbelliferone system HRP-III might be formed. Therefore, a more sophisticated spectral analysis was performed to evaluate the concentration of four HRP species. One micromolar solutions of native HRP, HRP-I, HRP-II, and HRP-III were prepared, and their absorption spectra were measured. HRP-I and HRP-II were prepared as described in section 2.3. HRP-III was prepared by the addition of excess H_2O_2 (10.2 mM) to native HRP. The spectra were digitized with a resolution 1 nm and stored in an ASCII file so that they were available for the spectra-analyzing program. The absorption spectra of HRP in the reaction mixture 0.1 mM IAA/1 μM HRP/1 μM

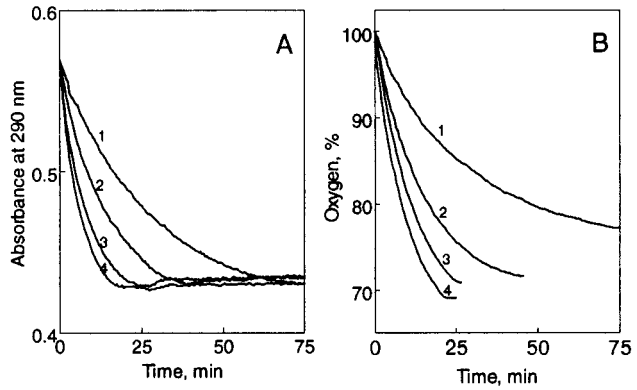

Figure 1. Influence of umbelliferone on the oxidation of 0.1 mM IAA catalyzed by 1 μM HRP, followed by absorbance of IAA at 290 nm (A) and by oxygen consumption (B). The concentrations of umbelliferone are 0 (1), 0.1 (2), 0.2 (3), and 0.3 μM (4).

umbelliferone were measured in the Soret (350−450 nm) and visible (500−600 nm) regions at different times after the reaction initiation. They were also digitized with a resolution 1 nm and put in an ASCII file. A program for the spectral analysis was designed by S.N.K. A model spectrum was calculated according to

$$A_{\mathrm{mod}}(\lambda) = \sum_{i=1}^{4} C_i \epsilon_i(\lambda) l \qquad (1)$$

where C_i and ϵ_i are the concentration and extinction coefficient for HRP species number i. $i = 1, 2, 3, 4$ represents four HRP species: native HRP, HRP-I, HRP-II, and HRP-III; l is an optical path length. The concentrations C_i were evaluated in an iteration procedure by minimization of the function

$$\sum_{\lambda} \{A_{\mathrm{exp}}(\lambda) - A_{\mathrm{mod}}(\lambda)\}^2 \qquad (2)$$

where $A_{\mathrm{exp}}(\lambda)$ is an experimentally measured spectrum of HRP species during IAA oxidation.

3. Results

3.1. Effect of Umbelliferone on IAA Oxidation. Umbelliferone caused an acceleration of HRP-catalyzed IAA oxidation which was detected by following the decrease in IAA absorption at 290 nm and by measuring oxygen consumption (Figure 1). We quantitate the extent of acceleration by umbelliferone by use of the ratio of the initial rate of IAA oxidation in the presence of umbelliferone to that in its absence. The acceleration increased with increasing [umbelliferone] up to a factor of 8 at [umbelliferone] = 1 μM (Figure 2). Further increase of [umbelliferone] did not influence the acceleration.

3.2. Effect of Umbelliferone on the Concentration of ROOH. Hydroperoxide is formed in a free radical chain reaction which constitutes part of the IAA oxidation mechanism.[6−8] Since umbelliferone increases the rate of IAA oxidation, it could result in an enhanced formation of hydroperoxide. In a previous paper we showed that the hydroperoxide concentration can be determined indirectly in the presence of inhibitor by measuring the critical inhibitor concentration required to cause an abrupt decrease in the rate of reaction: critical inhibitor concentration is about twice the hydroperoxide concentration.[7] We measured the critical concentration of inhibitor, caffeic acid, for the system 0.1 mM IAA/1 μM HRP in the absence and in the presence of 1 μM umbelliferone. Caffeic acid was added 90 s after reaction initiation in the 0.1 mM IAA/1 μM HRP system and 45 s after reaction initiation in the 0.1 mM IAA/1 μM HRP/1 μM umbelliferone system. The critical concentrations of caffeic acid were found to be 1.3 ± 0.3 μM without umbelliferone and 1.8 ± 0.3 μM in the presence of umbelliferone. We conclude that umbelliferone does not have a pronounced influence on the concentration of hydroperoxide during HRP-catalyzed IAA oxidation.

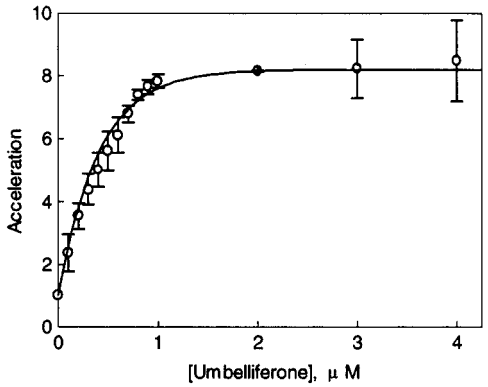

Figure 2. Accelerating effect of umbelliferone on the oxidation of 0.1 mM IAA catalyzed by 1 μM HRP. Acceleration is the ratio between the initial rate of IAA oxidation in the presence of umbelliferone and that in its absence. Each point on the plot is an average of three values obtained in three different ways: (1) by IAA depletion followed by absorption at 290 nm, (2) by IAA depletion measured with Salkowski reagent, and (3) by oxygen consumption measured with an oxygen electrode.

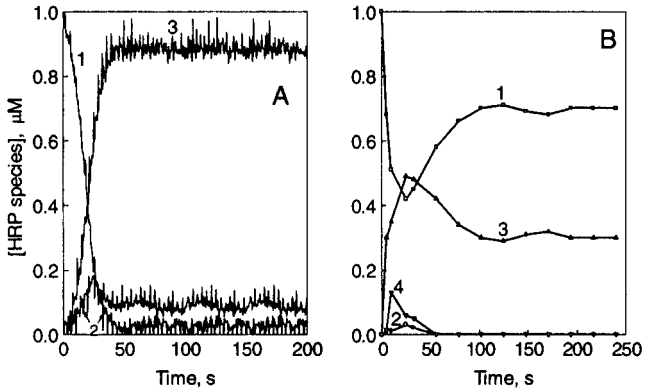

Figure 3. Concentrations of native HRP (1), HRP-I (2), HRP-II (3), and HRP-III (4) during the oxidation of 0.1 mM IAA catalyzed by 1 μM HRP without umbelliferone (A) and in the presence of 1 μM umbelliferone (B).

3.3. Effect of Umbelliferone on the Composition of HRP Species. No HRP-III was observed during IAA oxidation in the 0.1 mM IAA/1 μM HRP system at pH 7.4. Traces of HRP-I were detected only in the pre-steady state, whereas HRP-II is the predominant HRP intermediate in both the pre-steady state and the steady state (Figure 3A). The steady state of the HRP-catalyzed IAA oxidation is sustained for about 80 min for the above experimental conditions.[5] Spectral analysis (based on the assumption that four HRP species—native HRP, HRP-I, HRP-II, and HRP-III—were present in the reaction mixture; see section 2.6) indicated that only traces of HRP-I and HRP-III were formed in the presence of 1 μM umbelliferone during the presteady state (Figure 3B). HRP-II appeared to reach its maximal concentration of 0.5 μM in 25 s, then declined, and remained at the level of about 0.3 μM during the steady state. However, this interpretation could be incorrect. Figure 4 shows an example of experimentally determined and optimally modeled spectra. There are differences between the experimental and model spectra at 390−400 nm and in the visible region. The difference in the Soret region can be explained by the formation

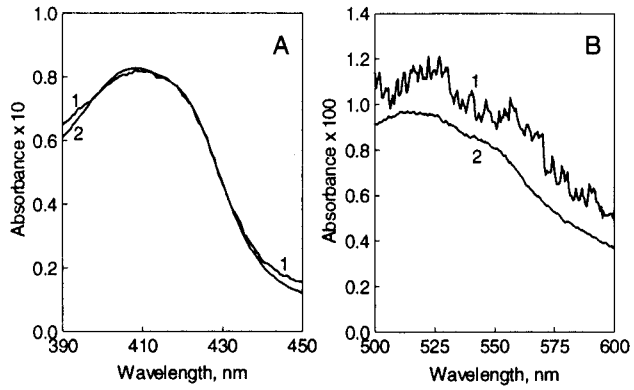

Figure 4. Spectral analysis of the HRP absorption spectrum obtained 33 s after reaction initiation in the 0.1 mM IAA/1 μM HRP/1 μM umbelliferone system. Plates A and B show Soret and visible spectral regions. Line 1 is an experimental spectrum whereas line 2 is an optimal model spectrum consisting of four components: 0.44 μM native HRP, 0.03 μM HRP-I, 0.48 μM HRP-II, and 0.05 μM HRP-III.

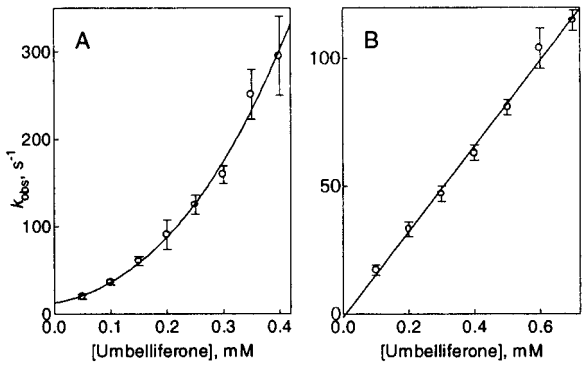

Figure 5. Plots of the pseudo-first-order rate constant, k_{obs}, versus [umbelliferone] for the reduction of HRP-I (A) and HRP-II (B) by umbelliferone.

of IAA oxidation products which absorb in this range, whereas the difference in the visible range (small, but perhaps significant) cannot be ascribed to the absorption of IAA oxidation products, nor to umbelliferone, nor to umbelliferone oxidation products, nor to the experimental errors. Therefore, it may be concluded that one of the HRP species formed in IAA/HRP/umbelliferone system differs from that in the absence of umbelliferone. Additional results giving rise to the same conclusion are discussed below (section 3.5).

P-670 is an inactive HRP species accumulated during the HRP-catalyzed IAA oxidation.[5,20] In the absence of umbelliferone the amount of P-670 formed in the 0.1 mM IAA/1 μM HRP system reached 0.6 μM,[5] while in the presence of 1 μM umbelliferone it was less than 0.2 μM (Figure 1S). Thus, umbelliferone significantly diminishes formation of P-670 during the HRP-catalyzed IAA oxidation.

3.4. Reduction of HRP-I and HRP-II by Umbelliferone. The plot of k_{obs} vs [umbelliferone] for the reduction of HRP-I by umbelliferone is shown in Figure 5A. The rate constant increases with increasing [umbelliferone]; at 350 μM it is 1.3 $\times$ 10^6 M^{-1} s^{-1}, about 6 times higher than that at 50 μM (2.3 $\times$ 10^5 M^{-1} s^{-1}). The experimental data were fit with a polynomial function. For 1 μM umbelliferone the rate constant was estimated by extrapolation of the polynomial to be $k_{14} = 1.1 \times 10^5$ M^{-1} s^{-1}. The results show that there is a self-accelerating effect of umbelliferone on the reduction of HRP-I.

The rate of reduction of HRP-II by umbelliferone is linearly dependent upon the concentration of umbelliferone (Figure 5B). The rate constant for this reaction, obtained from the slope of the line in Figure 5B, is $k_{15} = (1.68 \pm 0.05) \times 10^5$ M^{-1} s^{-1}. Absorption spectra obtained during the oxidation of umbelliferone in the steady state in the 0.1 mM umbelliferone/10 nM HRP/1 mM H_2O_2 system showed two isosbestic points at 300 and 392 nm (Figure 2S). This indicates that a single product of umbelliferone oxidation is formed. Therefore, the rate constant for HRP-II reduction by umbelliferone can also be determined in the steady state, since the reduction of HRP-II is the rate-limiting step in the reaction. Single-exponential kinetic curves for umbelliferone oxidation were observed at 325 nm in the 0.1 mM umbelliferone/10 nM HRP/1 mM H_2O_2 system. From the slope of the linear plot of k_{obs} vs [HRP] (data not shown), the rate constant $k_{15} = (1.73 \pm 0.05) \times 10^5$ M^{-1} s^{-1} was obtained. Thus, the value of the rate constant for HRP-II reduction by umbelliferone obtained from steady state kinetics is equal within experimental error to that obtained from the transient state.

3.5. Effect of Umbelliferone on the Reduction of HRP-I by IAA. The reduction of HRP-I by IAA in the presence of umbelliferone was followed in the transient state at 411 nm. Figure 6A shows the kinetic trace for the reduction of 1 μM HRP-I by 1 μM umbelliferone, Figure 6B the trace for the reduction of 1 μM HRP-I by 0.1 mM IAA, and Figure 6C that for the reduction of 1 μM HRP-I by the combination of 1 μM umbelliferone and 0.1 mM IAA. The rate constants k_{obs} were obtained from single-exponential fits of experimental kinetic traces.[29] Figure 7A shows the rate constants k_{obs} for the reduction of 1 μM HRP-I by 1 μM umbelliferone, by 0.1 mM IAA, and by 1 μM umbelliferone + 0.1 mM IAA. It is seen that the presence of the catalytic amount of umbelliferone results in a dramatic (factor of 10) acceleration of HRP-I reduction by IAA:

$$k_{obs}^{IAA+Umb} \approx 10(k_{obs}^{IAA} + k_{obs}^{Umb}) \quad (3)$$

The acceleration was not the only effect of umbelliferone on HRP-I reduction by IAA. Figure 7B shows the maximal change in absorbance at 411 nm during the reduction of 1 μM HRP-I by 1 μM umbelliferone, 0.1 mM IAA, and a mixture of both reducing substrates. It is seen that the changes of absorbance are equal for each substrate by itself but significantly lower for the combination of both substrates. Since the initial absorbances are equal for all three experiments, the final absorbance for the experiment with both substrates present is lower than that for single substrates. A possible explanation is that the product of HRP-I reduction by IAA (presumably HRP-II) is spectrally different in the presence of umbelliferone from that in its absence.

3.6. The Effect of Umbelliferone on the Reduction of HRP-II by IAA. The reduction of HRP-II by IAA in the presence of umbelliferone was also studied. Since HRP-II is rapidly regenerated in the presence of oxygen (because of the chain reaction), deoxygenated solutions were used (see section 2.3). It was found that

$$k_{obs}^{IAA+Umb} \approx k_{obs}^{IAA} + k_{obs}^{Umb} \quad (4)$$

that is, umbelliferone does not influence the reduction of HRP-II by IAA.

3.7. Examination of Umbelliferone Binding to Native HRP. A possible explanation of the striking data on both HRP-I reduction by umbelliferone and the effect of umbelliferone on the reduction of HRP-I by IAA is that there is binding of umbelliferone to HRP-I away from the active site, which somehow causes a catalytic effect. It is impossible to measure the binding of umbelliferone as a mediator of HRP-I reduction because umbelliferone is also a substrate of HRP-I. Therefore,

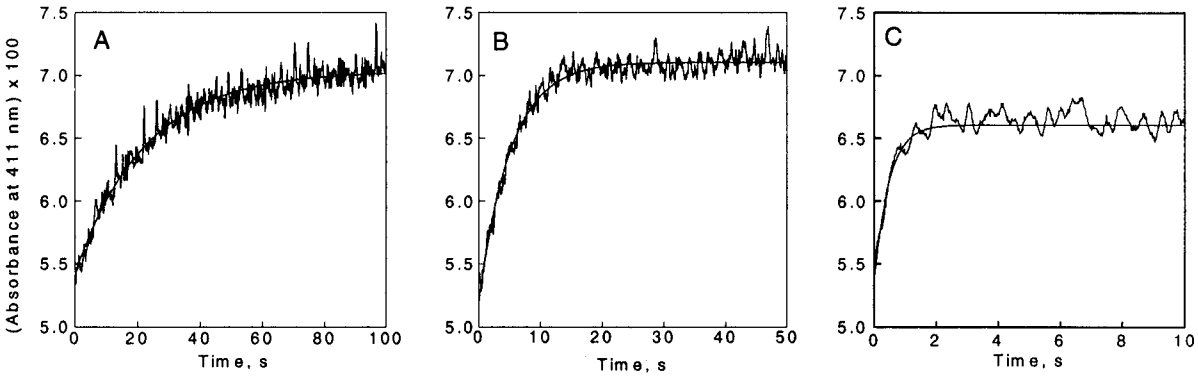

Figure 6. Kinetic traces for the reduction of 1 μM HRP-I by 1 μM umbelliferone (A), 0.1 mM IAA (B), and 1 μM umbelliferone + 0.1 mM IAA (C) followed at 411 nm.

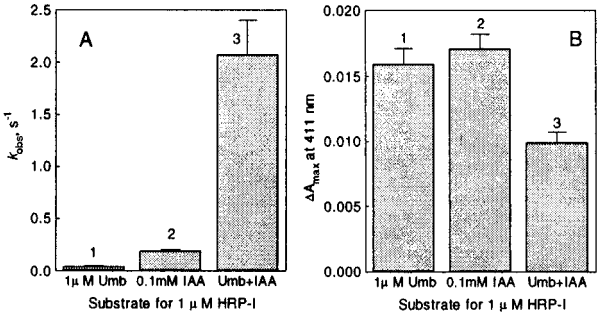

Figure 7. k_{obs} (A) and maximal change of absorbance at 411 nm (B) for the reduction of 1 μM HRP-I by 1 μM umbelliferone (column 1), 0.1 mM IAA (column 2), and 1 μM umbelliferone + 0.1 mM IAA (column 3).

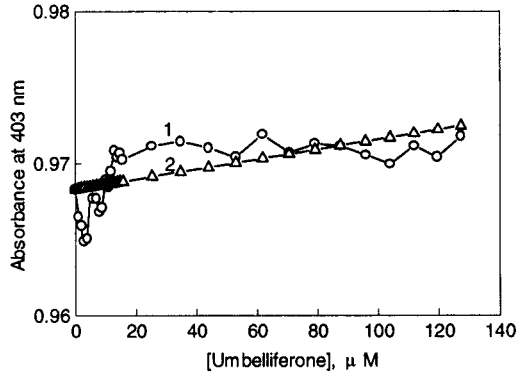

Figure 8. Titration of native HRP by umbelliferone: experimentally measured absorbance (1) and absorbance calculated by correcting for dilution and the additional effect of umbelliferone absorption (2).

we studied the effect of umbelliferone on the absorption of native HRP. Figure 8 shows experimental absorbance and calculated absorbance as functions of added umbelliferone. The theoretical line was calculated according to the following expression:

$$A = \frac{A_0 V_0 + [\mathrm{Umb}] V_{\mathrm{Umb}} \epsilon_{\mathrm{Umb}} l}{V_0 + V_{\mathrm{Umb}}} \qquad (5)$$

assuming that only HRP dilution and umbelliferone absorption contribute to the change of absorption when umbelliferone is added. In eq 5, A_0 and V_0 are the absorbance of HRP at 403 nm and the volume of HRP solution before umbelliferone addition, [Umb] is the concentration of umbelliferone in its stock solution, V_{Umb} is the volume of umbelliferone added, ϵ_{Umb} is the extinction coefficient of umbelliferone at 403 nm (1.0×10^3 $\mathrm{M^{-1}\ cm^{-1}}$), and l is the optical path length. The maximal deviation of the experimental curve from the calculated line does not exceed 0.5%, which is about the volume error occurring during umbelliferone injection. These results do not disprove the binding of umbelliferone to HRP-I; but they show that indirect evidence is lacking.

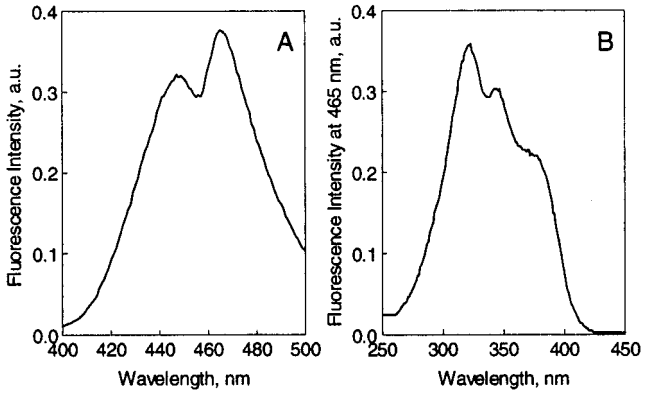

Figure 9. Fluorescence (A) and excitation (B) spectra of umbelliferone. Both spectra were measured using 10 μM umbelliferone in 0.1 M phosphate buffer pH 7.4. For plate A $\lambda_{ex} = 325$ nm.

3.8. Determination of the pK_a for Umbelliferone. Umbelliferone is intensively fluorescent with a maximal emission at 465 nm (Figure 9A). Hence, its fluorescence was used for determination of its pK_a value. The spectrum of excitation has a maximum at 325 nm (Figure 9B), which is in agreement with absorption spectrum (see Figure 2S). When the pH is changed, the shape of fluorescence spectrum is unchanged but the intensity of fluorescence is affected: the neutral form has more intensive fluorescence than the anionic one. Figure 3S shows the effect of pH on the fluorescence intensity (I). The following function was used for the nonlinear regression analysis of the experimental data I vs pH:

$$I = \frac{I_{\mathrm{min}} + I_{\mathrm{max}} \times 10^{(\mathrm{p}K_a - \mathrm{pH})}}{1 + 10^{(\mathrm{p}K_a - \mathrm{pH})}}$$

where I_{min}, I_{max}, and pK_a were variable parameters. The pK_a value obtained from this analysis was 7.78 ± 0.03.

4. Discussion

4.1. Mechanism of HRP-Catalyzed IAA Oxidation. The kinetics of the HRP-catalyzed oxidation of IAA at neutral pH are now well understood: enzymatic IAA oxidation in the standard peroxidase cycle is accompanied by a nonenzymatic free radical chain reaction.[5−8] In our previous papers we developed a model for the HRP-catalyzed IAA oxidation.[6−8] This model did not define the structures of the free radicals involved in the chain reaction.

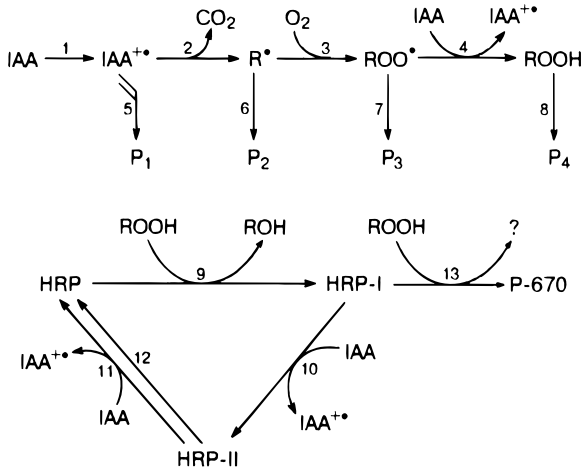

Figure 10. Detailed model of the HRP-catalyzed IAA oxidation at neutral pH: (top) a free-radical chain reaction; (bottom) HRP turnover.

TABLE 1: Main Reactions Involved in the HRP-Catalyzed Oxidation of IAA at pH 7.4 in the Absence of Umbelliferone (Reactions 1−13) and in the Presence of Umbelliferone (Reactions 14−16)

no.	reaction	rate constants	ref
1	IAA → IAA$^{\bullet+}$	$k_1 = 3 \times 10^{-7}$ s^{-1}	7
2	IAA$^{\bullet+}$ → R$^{\bullet}$ + CO_2	$k_2 = 90$ s^{-1}	23
3	R$^{\bullet}$ + O_2 → ROO$^{\bullet}$	$k_3 = 2.0 \times 10^8$ M^{-1} s^{-1}	23
4	ROO$^{\bullet}$ + IAA → ROOH + IAA$^{\bullet+}$	$k_4 = 1.0 \times 10^6$ M^{-1} s^{-1}	6
5	IAA$^{\bullet+}$ + IAA$^{\bullet+}$ → P_1	$2k_5 = 5.3 \times 10^8$ M^{-1} s^{-1}	23
6	R$^{\bullet}$ → P_2	$k_6 = 1.8 \times 10^4$ s^{-1}	6
7	ROO$^{\bullet}$ → P_3	$k_7 = 5.62$ s^{-1}	6
8	ROOH → P_4	$k8 = 1.45 \times 10^{-3}$ s^{-1}	2, 6
9	HRP + ROOH → HRP-I + ROH	$k_9 = 2.0 \times 10^6$ M^{-1} s^{-1}	2, 6
10	HRP-I + IAA → HRP-II + IAA$^{\bullet+}$	$k_{10} = 2.3 \times 10^3$ M^{-1} s^{-1}	5, 6
11	HRP-II + IAA → HRP + IAA$^{\bullet+}$	$k_{11} = 2.05 \times 10^2$ M^{-1} s^{-1}	5, 6
12	HRP-II → HRP	$k_{12} = 1.75 \times 10^{-3}$ s^{-1}	6
13	HRP-I + ROOH → P-670	$k_{13} = 6.2 \times 10^2$ M^{-1} s^{-1}	6
14	HRP-I + Umb → HRP-II + Umb$^{\bullet}$	$k_{14} = 1.1 \times 10^5$ M^{-1} s^{-1}	*a*
15	HRP-II + Umb → HRP + Umb$^{\bullet}$	$k_{15} = 1.7 \times 10^5$ M^{-1} s^{-1}	*a*
16	Umb$^{\bullet}$ + IAA → Umb + IAA$^{\bullet+}$	*b*	

[a] Present paper. [b] No data available.

The literature on free radical participation in IAA oxidation by HRP begins in 1956 and has been well reviewed.[30] However, it was not until 1986 that a free radical was detected by EPR. Mottley and Mason[30] trapped and identified the skatolyl radical in a system containing HRP, IAA, and H_2O_2 in acetate buffer at pH 4.6. In a later study by Escobar et al.,[31] using the same reactants, the skatolyl radical was also detected at pH 7.4. In remarkable recent studies by Candeias et al.[23,24] of one-electron oxidation of IAA, the IAA cation radical was detected, its acid−base properties were measured, and its rate of decarboxylation to form the skatolyl radical was determined.

Here we present our model, modified on the basis of the above results, so that all free radical species are identified. The major change in the kinetics is the incorporation of one additional elementary reaction, which is not rate controlling. This step is the decarboxylation of the IAA cation radical to form the skatolyl radical. The modified model is shown in Figure 10; corresponding reactions (reactions 1−13) and the rate constants are listed in Table 1. The notations IAA, IAA$^{\bullet+}$, R$^{\bullet}$, ROO$^{\bullet}$, ROOH, and ROH are used for the species shown in Figure 11.

Reaction 1 is a very slow nonenzymatic process responsible for the production of IAA$^{\bullet+}$ traces in the absence of HRP.[7] This reaction is important for the initiation of enzymatic oxidation (particularly in the presence of inhibitors) but does not play any significant role during the steady state of HRP-catalyzed IAA oxidation.[7] IAA$^{\bullet+}$ tends to deprotonate rapidly at neutral pH; however there is an equilibrium fraction of protonated IAA$^{\bullet+}$ which can decarboxylate to the skatolyl radical R$^{\bullet}$ (reaction 2).[7] R$^{\bullet}$, in turn, is rapidly scavenged by O_2 to form ROO$^{\bullet}$ (reaction 3).[23,24] ROO$^{\bullet}$ reacts with IAA producing IAA$^{\bullet+}$ and ROOH (reaction 4).[32] Reactions 5−8 are termination steps for the intermediates IAA$^{\bullet+}$, R$^{\bullet}$, ROO$^{\bullet}$, and ROOH.[6] It was shown that IAA$^{\bullet+}$ undergoes bimolecular radical−radical recombination (reaction 5),[23] whereas the termination steps for R$^{\bullet}$ and ROO$^{\bullet}$ and ROOH are satisfactorily described by the unimolecular reactions 6−8.[6] The reaction sequence 1−8 is a complex free radical chain process, producing two essential intermediates: IAA$^{\bullet+}$ and ROOH. Reactions 1−8 are responsible for the presence of ROOH traces in the IAA solution in the absence of HRP;[7] after HRP addition, these traces of ROOH initiate HRP participation in the reaction. During the steady state the reaction sequence 1−8 regenerates the hydroperoxide, ROOH, required for sustaining the enzymatic cycle.

IAA is oxidized in the standard peroxidase cycle (reactions 9−11). Two cation radicals required for sustaining the free radical chain are produced during one HRP turnover. HRP-II is slowly reduced in the absence of IAA (reaction 12).[5,6] Reaction 13 represents a rate-limiting step in P-670 formation.[5,6] The essence of the mechanism is that a trace of peroxide (ROOH) is all that required to initiate the reaction. The combination of the nonenzymatic free radical chain and the peroxidase cycle continually produce ample ROOH for the

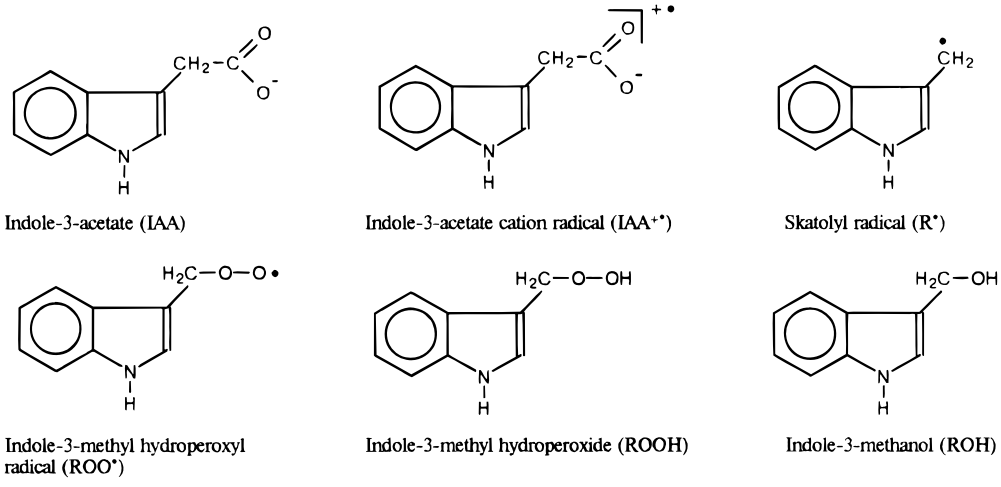

Figure 11. Structures of compounds and radicals, their names, and abbreviations.

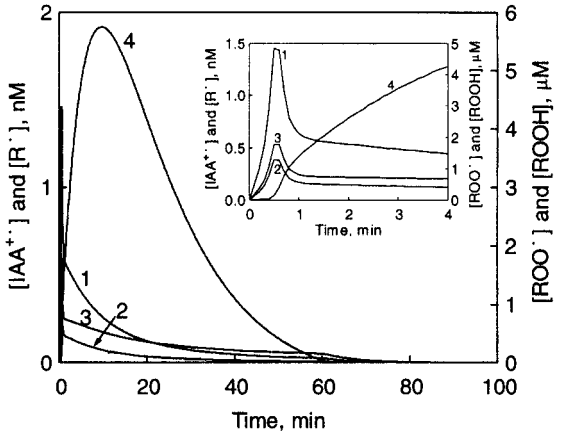

Figure 12. Simulated kinetic traces of intermediates: (1) $IAA^{\bullet+}$, (2) $R^{\bullet}$, (3) $ROO^{\bullet}$, and (4) ROOH during HRP-catalyzed IAA oxidation. Differential equations and parameters used for computer simulation are listed in Table 2.

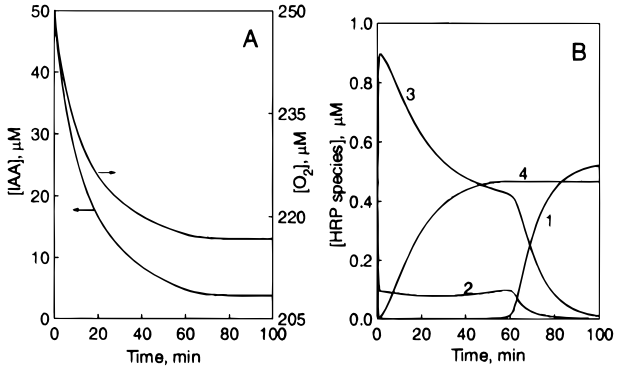

Figure 13. Simulated kinetic traces of substrates (A) and HRP species (B) during the HRP-catalyzed IAA oxidation. HRP species are (1) native HRP, (2) HRP-I, (3) HRP-II, and (4) P-670. Differential equations and parameters used for computer simulation are listed in Table 2.

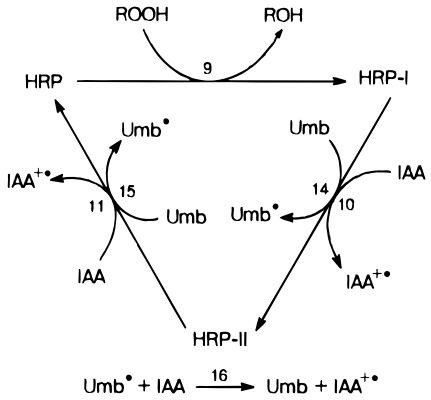

Figure 14. Reactions required to explain the accelerating effect of umbelliferone on the HRP-catalyzed IAA oxidation.

reaction to reach and maintain its maximal steady state rate, which is maintained until inactivation processes become dominant.

The present model was derived from that previously discussed[6,7] by adding reactions 2 and 5, the decarboxylation of $IAA^{\bullet+}$, and its formation of secondary products. The rate constants k_4, k_6−k_8, and k_{13} (see Table 1), obtained from computer simulation, might be affected by the modified model. Therefore, we carried out the computer simulation of the modified model, using software described elsewhere,[6] to examine the values of the above rate constants. Figures 12 and 13 show the simulated concentrations of all the intermediates, substrates, and HRP species. The simulated concentrations of

TABLE 2: Rate Equations and Parameters Used for Computer Simulation of the HRP-Catalyzed IAA Oxidation

Rate Equations

1. $d[IAA]/dt = -(k_1 + k_4[ROO^{\bullet}] + k_{10}[HRP\text{-}I] + k_{11}[HRP\text{-}II])[IAA]$
2. $d[IAA^{\bullet+}]/dt = (k_1 + k_4[ROO^{\bullet}] + k_{10}[HRP\text{-}I] + k_{11}[HRP\text{-}II])[IAA] - (k_2 + 2k_5[IAA^{\bullet+}])[IAA^{\bullet+}]$
3. $d[R^{\bullet}]/dt = k_2[IAA^{\bullet+}] - (k_3[O_2] + k_6)[R^{\bullet}]$
4. $d[O_2]/dt = -k_3[O_2][R^{\bullet}]$
5. $d[ROO^{\bullet}]/dt = k_3[O_2][R^{\bullet}] - (k_4[IAA] + k_7)[ROO^{\bullet}]$
6. $d[ROOH]/dt = k_4[ROO^{\bullet}][IAA] - (k_8 + k_9[HRP] + k_{13}[HRP\text{-}I])[ROOH]$
7. $d[HRP]/dt = (k_{11}[IAA] + k_{12})[HRP\text{-}II] - k_9[HRP][ROOH]$
8. $d[HRP\text{-}I]/dt = k_9[HRP][ROOH] - (k_{10}[IAA] + k_{13}[ROOH])[HRP\text{-}I]$
9. $d[HRP\text{-}II]/dt = k_{10}[HRP\text{-}I][IAA] - (k_{11}[IAA] + k_{12})[HRP\text{-}II]$
10. $d[P\text{-}670]/dt = k_{13}[HRP\text{-}I][ROOH]$

Initial Concentrations

$[HRP]_0 = 1\ \mu M$ $[ROOH]_0 = 2.7 \times 10^{-4}[IAA]_0$[7]
$[IAA]_0 = 50\ \mu M$ all other initial concentrations are zero
$[O_2]_0 = 250\ \mu M$[27]

Integration Parameters

step size lower limit = 0 step size error = 1×10^{-2}

all the species, except $IAA^{\bullet+}$ and $R^{\bullet}$, are the same for modified and nonmodified models (see Figures 5 and 6 in ref 6). Thus, the modified model is in good agreement with the experimental kinetics.[6] With regard to the concentrations of $IAA^{\bullet+}$ and $R^{\bullet}$, their sum for the modified model is simply equal to the concentration of $R^{\bullet}$ in the original model.

The model depicted in Figure 10 is the most realistic and comprehensive model of HRP-catalyzed IAA oxidation at neutral pH presently available. All the rate constants were either experimentally measured or determined in a computer simulation. The model satisfactorily describes most of the available experimental facts.

4.2. Mechanisms of Accelerating Effect of Umbelliferone on the HRP-Catalyzed IAA Oxidation. Phenols are known to be positive effectors of peroxidase-catalyzed reactions.[25,33,34] Three possible mechanisms of acceleration are examined: (1) the phenol-induced reduction of compound II (rate-limiting peroxidase species) to native enzyme, which results in increasing the rate of enzymatic oxidation of a substrate,[33,34] (2) the nonenzymatic oxidation of a substrate by a phenol free radical (formed in HRP-catalyzed phenol oxidation), which does not increase the rate of enzymatic substrate oxidation,[35,36] and (3) the allosteric effect of phenols, changing the conformation of HRP in a favorable way.[37] Here we consider all three possible mechanisms with respect to umbelliferone-induced acceleration of HRP-catalyzed IAA oxidation.

Phenols react as hydrogen atom donors to the oxidized peroxidase compounds.[33,34] Since the pK_a value for umbelliferone (7.78) is close to the pH used for the present studies (7.4), the umbelliferone reaction mixtures contain about 50% of the ionized form, which would be unreactive.

4.2.1. Reduction of Rate-Limiting HRP Species. Umbelliferone is oxidized by HRP-I and HRP-II (see section 3.3). Its involvement in the enzymatic cycle is represented by reactions 14 and 15 in Figure 14. Since umbelliferone influences the overall rates of HRP-I and HRP-II reduction, it influences the steady state concentrations of HRP, HRP-I, and HRP-II according to

$$[HRP] = \frac{[HRP]_0}{1 + \dfrac{k_9[ROOH]}{k_{10}[IAA] + k_{14}[Umb]} + \dfrac{k_9[ROOH]}{k_{11}[IAA] + k_{15}[Umb]}} \quad (6)$$

$$[\text{HRP-I}] = \frac{[\text{HRP}]_0}{1 + \dfrac{k_{10}[\text{IAA}] + k_{14}[\text{Umb}]}{k_{11}[\text{IAA}] + k_{15}[\text{Umb}]} + \dfrac{k_{10}[\text{IAA}] + k_{14}[\text{Umb}]}{k_9[\text{ROOH}]}} \quad (7)$$

$$[\text{HRP-II}] = \frac{[\text{HRP}]_0}{1 + \dfrac{k_{11}[\text{IAA}] + k_{15}[\text{Umb}]}{k_{10}[\text{IAA}] + k_{14}[\text{Umb}]} + \dfrac{k_{11}[\text{IAA}] + k_{15}[\text{Umb}]}{k_9[\text{ROOH}]}} \quad (8)$$

The above expressions were obtained using reactions 9−15 that are directly involved in HRP turnover (see Figure 14) and the assumption that [HRP], [HRP-I], and [HRP-II] are constant in the steady state. The rate of IAA oxidation in the enzymatic cycle is

$$\text{d[IAA]/d}t = -k_{10}[\text{HRP-I}][\text{IAA}] - k_{11}[\text{HRP-II}][\text{IAA}] \quad (9)$$

Using eqs 7−9, we calculated the acceleration of IAA oxidation by 1 μM umbelliferone. The acceleration is defined as the ratio between d[IAA]/dt in the presence of umbelliferone and in its absence. The following concentrations were used in the calculation: [IAA] = 0.1 mM, $[\text{HRP}]_0 = 1$ μM, and [ROOH] = 6 μM. The value of [ROOH] used in the calculations corresponds to that estimated for the steady state of HRP-catalyzed IAA oxidation in the absence of umbelliferone.[6,7] Our experiments showed that the presence of umbelliferone did not influence significantly the concentration of [ROOH] (see section 3.1). Moreover, numerical analysis of eqs 7−9 showed that the acceleration is not sensitive to the value of [ROOH] over a wide range. For the rate constants listed in Table 1 the maximal acceleration was equal to 2.5, which is much less than the value of 8 observed experimentally (see Figure 2). Even if it is assumed that $k_{14} = 0$, so that all reacted umbelliferone reduces compound II, the maximal acceleration is only a factor of 3, which is much less than the experimental value. Therefore, the reduction of HRP-II alone cannot explain accelerating effect of umbelliferone on the HRP-catalyzed IAA oxidation.

The concentration of umbelliferone was 2 orders of magnitude less than that of IAA. Reactions 14 and 15 result in very fast oxidation of umbelliferone. If there is no umbelliferone regeneration, then all of it is oxidized in the first few seconds. In contrast, umbelliferone-induced acceleration was observed over several minutes.

4.2.2. IAA Oxidation by the Free Radical of Umbelliferone. The free radicals of umbelliferone formed in reactions 14 and 15 are able, in principle, to participate in reaction 16. This reaction provides us with a mechanism of umbelliferone regeneration needed to explain the prolonged accelerating effect. Moreover, reaction 16 itself can contribute to acceleration of IAA oxidation. Since reaction 16 requires the formation of umbelliferone free radicals (reactions 14 and 15), the accelerating effect of both reactions 15 and 16 must be considered together. Thus, we are now examining the cumulative effect of acceleration caused by compound II reduction and of umbelliferone free radicals.

To estimate the accelerating effect of reactions 14−16, we assume that (i) the steady state for reactions 9−16 (Figure 13) is established (the concentrations of HRP, HRP-I, HRP-II, Umb, and Umb$^\bullet$ are constants) and (ii) reaction 16 is fast enough that the steady state concentration of umbelliferone is much higher than that of its radical. These assumptions allow us to estimate maximal possible acceleration of IAA oxidation provided by the addition of reactions 14−16 to reactions 9−11. Using the above assumption we obtained the rate of IAA oxidation in reactions 10, 11, and 16:

$$\text{d[IAA]/d}t = -k_{10}[\text{HRP-I}][\text{IAA}] - k_{11}[\text{HRP-II}][\text{IAA}] - k_{14}[\text{HRP-I}][\text{Umb}] - k_{15}[\text{HRP-II}][\text{Umb}] \quad (10)$$

Using eqs 7, 9, and 10, as well as the rate constants k_9−k_{15} listed in Table 1, and the concentrations [IAA] = 0.1 mM, $[\text{HRP}]_0 = 1$ μM, and [ROOH] = 6 μM, we calculated maximal possible accelerating effect of 1 μM umbelliferone to be about 6.4. The value calculated is still less than that obtained experimentally (see Figure 2). Thus, the steady state analysis shows that reduction of HRP-I and HRP-II by umbelliferone (reactions 14 and 15) together with the oxidation of IAA by the free radical of umbelliferone (reaction 16) still cannot account for the experimentally observed acceleration factor.

The low reactivity of umbelliferone radicals with IAA can be explained thermodynamically. The reduction potential of IAA radicals is 0.922 V at pH 7.4,[24] and that of umbelliferone is 0.315 V at pH 13.5.[38] The reduction potential of umbelliferone radicals can be calculated at pH 7.4 using the following expression:[39]

$$E_{\text{pH}_1} = E_{\text{pH}_2} + \frac{RT}{F}\ln\left(\frac{10^{-\text{p}K_a} + 10^{-\text{pH}_1}}{10^{-\text{p}K_a} + 10^{-\text{pH}_2}}\right) \quad (11)$$

where E_{pH_1} is the unknown reduction potential at pH_1, E_{pH_2} is the known reduction potential at pH_2, R is the gas constant, T is the absolute temperature, and F the Faraday constant. The pK_a of umbelliferone is 7.78 (section 3.8) and the pK_a of IAA is 5.09.[24] The result is a reduction potential of 0.346 V for umbelliferone at pH 7.4. From the Nernst equation

$$K = \text{e}^{\text{F}\Delta E/RT} \quad (12)$$

the equilibrium constant for reaction 16 is estimated to be 1.8×10^{-10}. Thus, it appears that reaction 16 is not an effective pathway for IAA oxidation and indicates the importance of the allosteric effect of umbelliferone on HRP.

4.2.3. Allosteric Effect of Umbelliferone on HRP. It is known that HRP can bind some phenols at more than one site.[37] Phenol bound away from the active site cannot be oxidized but can favorably change the conformation of HRP so that the rate of substrate oxidation is increased. Our experiments showed that umbelliferone increased the rate of HRP-I reduction by IAA by a factor of 10 but did not influence the rate of HRP-II reduction by IAA. HRP-I is not a rate-limiting HRP species; therefore, umbelliferone-induced acceleration of the HRP-I reduction by an order of magnitude cannot result in acceleration of the overall rate of IAA oxidation by a factor of 10. However, the umbelliferone-induced increase in the rate constant k_{10} does result in considerable increase in the rate of IAA oxidation. The increased reactivity of HRP-I would mean that the steady state concentration of HRP-I is lowered. Since P-670 is formed from reaction of ROOH with HRP-I, the smaller concentration of the latter would account for the decreased rate of P-670 formation.

We calculated the total accelerating effect of 1 μM umbelliferone on HRP-catalyzed IAA oxidation using eqs 7, 9, and 10 and the rate constants k_9 and k_{11}−k_{15} listed in Table 1, as well as $k_{10} = 2.3 \times 10^4$ M^{-1} s^{-1}, which accounts for the enhancing effect of umbelliferone on HRP-I reduction by IAA. The calculations were made for the following concentrations: [IAA] = 0.1 mM, $[\text{HRP}]_0 = 1$ μM, and [ROOH] = 6 μM. The maximal possible acceleration by all three mechanisms was calculated to be about 9.3. Taking into account that this value

is an upper limit of acceleration, we can conclude that it is in good agreement with experimentally observed value of 8. Thus, a combination of all three effects—the reduction of HRP-II by umbelliferone, oxidation of IAA by free radicals of umbelliferone, and umbelliferone-induced acceleration of HRP-I reduction by IAA—can explain umbelliferone-induced acceleration of overall IAA oxidation catalyzed by HRP.

5. Concluding Remarks

To summarize, umbelliferone accelerates the HRP-catalyzed IAA oxidation due to combination of three accelerating effects: (i) the reduction of the rate-limiting HRP species, HRP-II, by umbelliferone, which increases the rate of enzymatic IAA oxidation, (ii) nonenzymatic oxidation of IAA by free radicals of umbelliferone formed in the HRP-catalyzed oxidation of umbelliferone, and (iii) umbelliferone-induced acceleration of HRP-I reduction by IAA. Quantitative contributions of all three effects are similar.

Further development of this research should involve a detailed experimental investigation of the mechanisms of umbelliferone-induced acceleration of the HRP-I reduction by IAA as well as by umbelliferone itself. Moreover, further progress in detailed modeling requires the knowledge of the rate constant k_{16} as well as the rate constant of umbelliferone free radical recombination:

$$\mathrm{Umb}^{\bullet} + \mathrm{Umb}^{\bullet} \rightarrow \text{products}$$

Acknowledgment. This research was supported by the Natural Sciences and Engineering Research Council of Canada.

Supporting Information Available: Figures showing spectra of the formation of P-670 during oxidation of IAA and of umbelliferone oxidized by HRP as well as a graph of intensity of umbelliferone fluorescence vs pH (2 pages). Ordering information is given on any current masthead page.

References and Notes

(1) Abbreviations used were the following: IAA, indole-3-acetate; $IAA^{\bullet+}$, cation radical of IAA; $R^{\bullet}$, skatolyl radical; $ROO^{\bullet}$; indole-3-methylhydroperoxyl radical; ROOH, indole-3-methyl hydroperoxide; ROH, indole-3-methanol; HRP, HRP-I, HRP-II, and HRP-III are native form, compound I, compound II, and compound III of horseradish peroxidase; P-670, inactive verdohemoprotein; Umb, umbelliferone; $Umb^{\bullet}$, free radical of umbelliferone.

(2) Nakajima, R.; Yamazaki, I. *J. Biol. Chem.* **1979**, *254*, 872.

(3) (a) Smith, A. M.; Morrison, W. L.; Milham P. J. *Biochemistry* **1982**, *21*, 4414. (b) Ricard, J.; Job, D. *Eur. J. Biochem.* **1974**, *44*, 359.

(4) Metodiewa, D.; de Melo, M. P.; Escobar, J. A.; Cilento, G.; Dunford, H. B. *Arch. Biochem. Biophys.* **1992**, *296*, 27.

(5) Krylov, S. N.; Dunford, H. B. *Biophys. Chem.* **1996**, *58*, 325.

(6) Krylov, S. N.; Dunford, H. B. *J. Phys. Chem.* **1996**, *100*, 916.

(7) Krylov, S. N.; Dunford, H. B. *Photochem. Photobiol.* **1996**, *63*, 735.

(8) Krylov, S. N.; Dunford, H. B. In *Plant Peroxidases. Biochemistry and Physiology. IV International Symposium*; Obinger, C., Burner, U., Ebermann, R., Penel, C., Greppin, H., Eds.; University of Geneva: Geneva, 1996; pp 59−69.

(9) (a) Olson, D. L.; Scheeline, A. *J. Phys. Chem.* **1995**, *99*, 1204. (b) Olson, D. L.; Scheeline, A. *J. Phys. Chem.* **1995**, *99*, 1212. (c) Olson, D. L.; Williksen, E. P.; Scheeline, A. *J. Am. Chem. Soc.* **1995**, *117*, 2.

(10) Odajima, T.; Yamazaki, I. *Biochim. Biophys. Acta* **1970**, *206*, 71.

(11) Cilento, G.; Adam, W. *Photochem. Photobiol.* **1988**, *48*, 361.

(12) Krylov, S. N.; Aguda, B. D.; Ljubimova, M. L. *Biophys. Chem.* **1995**, *55*, 213.

(13) Krylov, S. N.; Lazarev, V. V.; Rubin, L. B. *Dokl. Biophys.* **1990**, *310*, 28.

(14) de Melo, M. P.; Escobar, J. A.; Metodiewa, D.; Dunford, H. B.; Cilento, G. *Arch. Biochem. Biophys.* **1992**, *296*, 34.

(15) Krylov, S. N.; Chebotareva, A. B. *FEBS Lett.* **1993**, *324*, 6.

(16) Davies, P. J. In *Plant Hormones: Physiology, Biochemistry and Molecular Biology*; Davies, P. J., Ed.; Kluwer Academic: Dordrecht, 1995; pp 4−5.

(17) Bandurski, R. S.; Cohen, J. D.; Slovin, J.; Reinecke, D. M. In *Plant Hormones: Physiology, Biochemistry and Molecular Biology*; Davies, P. J., Ed.; Kluwer Academic: Dordrecht, 1995; pp 39−65.

(18) Cleland, R. E. In *Plant Hormones: Physiology, Biochemistry and Molecular Biology*; Davies, P. J., Ed.; Kluwer Academic: Dordrecht, 1995; pp 214−227.

(19) Kobayashi, S.; Sugioka, K.; Nakano, H.; Nakano, M.; Tero-Kubota, S. *Biochemistry* **1984**, *23*, 4589.

(20) Nakajima, R.; Yamazaki, I. *J. Biol. Chem.* **1980**, *255*, 2067.

(21) Acosta, M.; Arnao, M. B.; Del Rio, J. A.; Garcia-Canovas, F. *Biochim. Biophys. Acta* **1989**, *996*, 7.

(22) Gazaryan, I. G.; Lagrimini, L. M.; Ashby, G. A.; Thorneley, N. F. *Biochem. J.* **1996**, *313*, 841.

(23) Candeias, L. P.; Folkes, L. K.; Dennis, M. F.; Patel, K. B.; Everett, S. A.; Stratford, M. R. L.; Wardman, P. *J. Phys. Chem.* **1994**, *98*, 10131.

(24) Candeias, L.; Folkes, L. K.; Porssa, M.; Parrick, J.; Wardman, P. *Biochemistry* **1996**, *35*, 102.

(25) Polevoi, V. V. *Phytohormones* (in Russian); St. Petersburg University Publishing: St. Petersburg, 1982; pp 89−91.

(26) Ohlsson, P.-I.; Paul, K.-G. *Acta Chem. Scand.* **1976**, *B30*, 373.

(27) Robinson, J.; Cooper, J. M. *Anal. Biochem.* **1970**, *33*, 390.

(28) Sacher, J. A. *Am. J. Bot.* **1961**, *48*, 820.

(29) Usually a single-exponential fit is performed when the conditions are pseudo-first-order. However, our study of the reduction of HRP-I by umbelliferone was conducted under non-pseudo-first-order conditions since the concentrations of HRP-I and umbelliferone were equal. Such a low concentration of umbelliferon was used because it was standard throughout the paper. Therefore, we performed a special investigation to prove that even far from pseudo-first-order conditions a single-exponential fit, with a floating end point, did not result in significant error in the rate constant k_{obs}. We simulated the kinetic trace of HRP-I reduction by an equimolar amount of umbelliferone. A single-exponential fit to the kinetic trace gave a k_{obs} value which differed only about 10% from the product of the bimolecular rate constant and initial concentration of umbelliferon used in the simulation. Therefore, the deviation of experimental conditions from pseudo-first-order does not prevent a relatively precise estimation of k_{obs}.

(30) Mottley, C.; Mason, R. P. *J. Biol. Chem.* **1986**, *261*, 16860.

(31) Escobar, J. A.; Vásquez-Vivar, J.; Cilento, G. *Photochem. Photobiol.* **1992**, *55*, 895.

(32) The stoichiometry requires that hydrogen atom transfer occurs. However, the $IAA^{\bullet+}$ cation radical is in rapid equilibrium with its conjugate base,[23] and since it is the cation radical which decarboxylates to form the skatolyl radical, we show it as the product.

(33) Marquez, L. A.; Dunford, H. B. *Arch. Biochem. Biophys.* **1993**, *305*, 414.

(34) Hsuanyu, Y.; Dunford, H. B. *J. Biol. Chem.* **1992**, *267*, 17649.

(35) Hodgson, M.; Jones, P. *J. Biolumin. Chemilumin.* **1989**, *3*, 21.

(36) Vlasenko, S. B.; Arefyev, A. A.; Klimov, A. D.; Kim, B. B.; Gorovits, E. L.; Osipov, A. P.; Gavrilova, E. M.; Egorov, A. M. *J. Biolumin. Chemilumin.* **1989**, *4*, 164.

(37) Critchlow, J. E.; Dunford, H. B. *J. Biol. Chem.* **1972**, *247*, 3703.

(38) Steenken, S.; Neta, P. *J. Phys. Chem.* **1982**, *86*, 3361.

(39) Wardman, P. *J. Phys. Chem. Ref. Data* **1989**, *18*, 1637.

JP962493T